

Stripe Conductivity in $\text{La}_{1.775}\text{Sr}_{0.225}\text{NiO}_4$

Yu.G.Pashkevich,¹ V.A.Blinkin,² V.P.Gnezdilov,³ V.V.Tsapenko,³ V.V.Eremenko,³ P.Lemmens,⁴ M.Fischer,⁴ M.Grove,⁴ G.Güntherodt,⁴ L.Degiorgi,⁵ P.Wachter,⁵ J.M.Tranquada,⁶ and D.J.Buttrey⁷

¹*A.A.Galkin Donetsk Physstech NASU, 83114 Donetsk, Ukraine*

²*Inst. for Single Crystals NASU, 310001 Kharkov, Ukraine*

³*B.I. Verkin Inst. for Low Temp. Physics NASU, 310164 Kharkov, Ukraine*

⁴*Physikalisches Institut, RWTH Aachen, 52056 Aachen, Germany*

⁵*Laboratorium für Festkörperphysik, ETH-Zürich, CH-8093, Zürich, Switzerland*

⁶*Brookhaven National Laboratory, Upton, NY 11973*

⁷*University of Delaware, Newark, Delaware 19716*

(August 10, 2018)

We report Raman light-scattering and optical conductivity measurements on a single crystal of $\text{La}_{1.775}\text{Sr}_{0.225}\text{NiO}_4$ which exhibits incommensurate charge-stripe order. The extra phonon peaks induced by stripe order can be understood in terms of the energies of phonons that occur at the charge-order wave vector, \mathbf{Q}_c . A strong Fano antiresonance for a Ni-O bond-stretching mode provides clear evidence for finite dynamical conductivity within the charge stripes.

71.45.Lr, 75.30.Fv, 78.30.Hv, 63.20.Kr

Recent experiments have shown a difference in the conductivity behavior of the stripe ordered phases in the cuprates $\text{La}_{2-x-y}\text{Nd}_x\text{Sr}_y\text{CuO}_4$ and the nickelates $\text{La}_{2-x}\text{Sr}_x\text{NiO}_4$. Strong localization and binding of charges to the lattice in nickelates manifest themselves by the appearance of: 1) an insulating state and a charge gap in optical conductivity [1,2]; and 2) additional diffraction peaks due to ionic displacements that are induced below T_c , the charge ordering temperature [3–5]. In cuprates such a gap is not observed [6] even though charge-order superlattice peaks have been detected by both neutron and x-ray scattering [7]. The diffraction measurements have shown that the corresponding lattice modulation is much smaller in cuprates than in nickelates [8,9]. At the same time both cuprates and nickelates have demonstrated incommensurate magnetic ordering [7,10,11]. This by itself is important evidence of the stripe state because it implies a modulation of the charge density. Moreover, the coexistence of superconductivity and stripe order has been observed in $\text{La}_{1.6-x}\text{Nd}_{0.4}\text{Sr}_x\text{CuO}_4$ with $x = 0.12, 0.15, \text{ and } 0.20$ [12,13].

The problem of whether or not stripes in cuprates and nickelates are insulating or metallic is fundamental to the physics of the stripe state. One can expect two possible scenarios which could lead to conductivity in the stripe state. According to the first one the stripes themselves are insulating but the system can be metallic due to fluctuations and motion of stripes [14]. Alternatively, metallic conductivity may exist along the charge threads without a violation of stripe ordering as a whole. In the latter case, Coulomb interactions between neighboring stripe should lead to charge-density-wave order along the stripes at sufficiently low temperatures and in the absence of stripe fluctuations [15].

Previous studies have shown that the stripe-order in

$\text{La}_{2-x}\text{Sr}_x\text{NiO}_4$ with $x = \frac{1}{3}$ has a short-period commensurability [5] and a very large charge gap of 0.26 eV relative to the charge ordering temperature of 230 K [2]. Thermodynamic measurements have indicated that $x = \frac{1}{3}$ may be somewhat special [16], while recent phonon density-of-states measurements have found doping-dependent changes of the in-plane Ni-O bond-stretching modes for $x = \frac{1}{4}, \frac{1}{3}, \text{ and } \frac{1}{2}$ [17]. Here we present results from Raman light scattering (RLS) and optical conductivity measurements on a single crystal with $x = 0.225$, which was previously characterized by neutron [10] and x-ray [11] diffraction. The stripe order in this sample is incommensurate, and the hole density per Ni site along a stripe is significantly less than 1 (in contrast to $x = \frac{1}{3}$, where the density is exactly 1). We observe a strong Fano antiresonance in the optical conductivity at an energy well below the charge pseudo-gap, which is 0.105 eV at 10 K. From a careful analysis of the phonon spectra, we conclude that the energy of the antiresonance corresponds to Ni-O bond stretching motions along the stripes. It follows that the antiresonance, which results from electron-phonon coupling, provides strong evidence for finite conductivity along the stripes, at least at optical-phonon frequencies.

The light scattering measurements were carried out in quasi-backscattering geometry using 514.5-nm argon laser light. The incident laser beam of 10 mW or 15 mW power was focused onto a 0.1 mm diameter spot on the a - b plane of the mirror-like polished crystal surface. The x, y, z - crystallographic axes in the $I4/mmm$ setting were determined by x-ray Laue diffraction. The incident photons were polarized along or perpendicular to the $x' = x + y$, or $y' = -x + y$ diagonal directions between in-plane Ni-O bonds. The scattered photons were polarized either parallel or perpendicular to the incident photons. Infrared (IR) reflectivity measurements in the

25–10⁵ cm⁻¹ frequency region were carried out in the geometry of normal incidence to the *a-b* plane of the sample. Optical conductivity spectra, $\sigma(\omega)$, were obtained by Kramers-Kronig analysis of the reflectivity data.

Let us begin with the optical conductivity spectra shown in Fig. 1. The conductivity below 2000 cm⁻¹ clearly decreases as the temperature is lowered. If we linearly extrapolate the frequency dependence from above 1500 cm⁻¹, as indicated by the dashed line for the 10 K spectrum, then, following Katsufuji *et al.* [2], we estimate a low-temperature gap of 840 cm⁻¹. At 150 K, which is the charge ordering temperature (T_c) indicated by diffraction [10,11], the conductivity has changed little. The extrapolated gap reaches zero somewhat closer to 200 K. Note that at low temperature, although $\sigma(0) \approx 0$, the residual conductivity within the extrapolated gap is significantly higher than that found for $x = \frac{1}{3}$ [2].

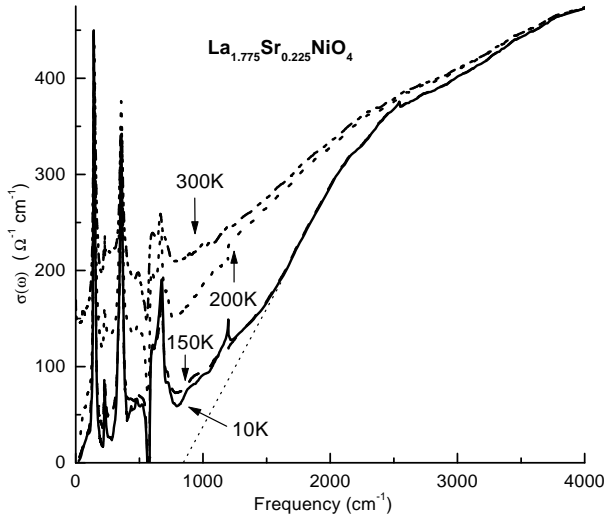


FIG. 1. The temperature dependence of the optical conductivity spectra of La_{1.775}Sr_{0.225}NiO₄ below 4000 cm⁻¹ for incidence normal to the *a-b* plane.

The temperature-dependent Raman spectra for two polarizations are presented in Fig. 2. For both *x'x'* and *x'y'* polarizations there is a significant electronic background that shifts from low to high energy as the temperature decreases. Low-temperature scans in the *x'y'* geometry reveal 2-magnon scattering bands at 739 cm⁻¹ and 1130 cm⁻¹, frequencies remarkably similar to those in La_{5/3}Sr_{1/3}NiO₄ [18,19]. For both $x = 0.225$ and $x = \frac{1}{3}$, the 2-magnon features disappear at approximately the charge-ordering temperature determined by neutron diffraction, 150 K and 240 K, respectively [5,10]. Analysis of the 2-magnon spectra will be presented elsewhere.

Next we consider the phononic features. In Fig. 2, the numeric labels denote the positions of lines (in cm⁻¹) at low temperature, determined by curve fitting. An expanded view of the low-frequency range of the optical

conductivity is shown in Fig. 3; again, the numbers label low-temperature peak positions.

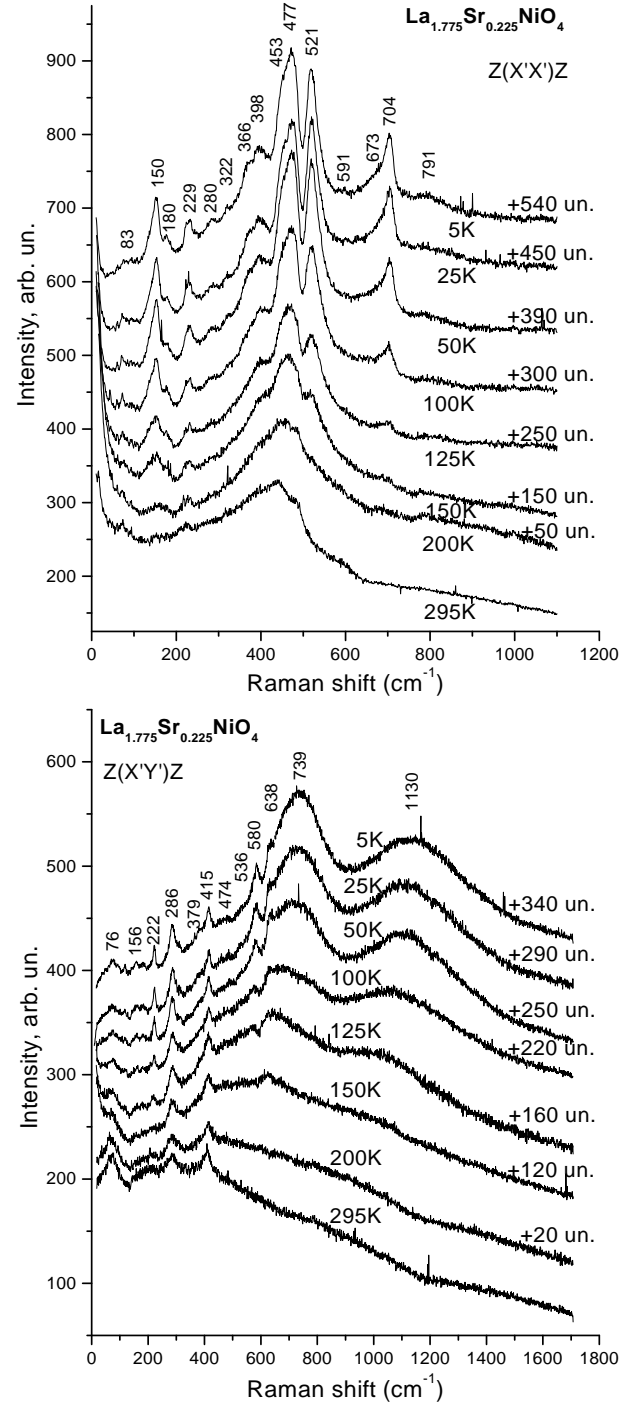


FIG. 2. Temperature dependent Raman light scattering spectra for *x'x'* and *x'y'* polarization of single crystal La_{1.775}Sr_{0.225}NiO₄. The vertical offsets are noted on the right.

To interpret the spectra, we begin by noting that RLS and IR measurements are sensitive only to modes with momentum transfer $\hbar Q = 0$. One certainly expects a significant contribution from optically-active phonon modes corresponding to the average lattice structure. In addi-

tion, the occurrence of stripe order, with a characteristic wave vector \mathbf{Q}_c , lowers the translational symmetry, and must lead to the appearance of extra lines in the RLS and IR spectra. Finally, the Sr dopant ions locally break the lattice symmetry, and hence can induce extra features, which are expected to be temperature independent.

The symmetry of the mean tetragonal lattice is described by space group $I4/mmm$. The corresponding Raman-active phonons are distributed among the irreducible representations (IREPs) of the space group as $2A_{1g}(153, 447) + 2E_g(90, 250)$, where the numbers in parentheses are phonon frequencies (in cm^{-1}) determined for La_2NiO_4 by neutron scattering [20]. The A_{1g} lines are allowed in the $x'x'$ geometry, and none are allowed in $x'y'$. The native IR-active phonon lines are represented as $3A_{2u}(346, 436, 490) + 4E_u(150, 220, 347, 654)$. Experimentally, the A_{1g} and E_u modes have been observed in previous RLS [21,22] and FIR [23,24] studies, respectively, on undoped La_2NiO_4 , and the frequencies obtained are in good agreement with the neutron results [20]. Features at similar frequencies are also prominent in measurements on our $x = 0.225$ sample, as can be seen in Figs. 2 and 3.

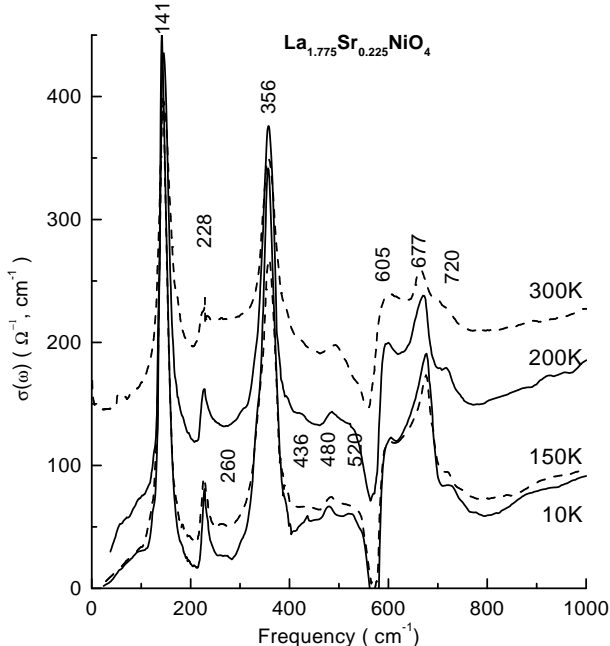


FIG. 3. Temperature dependence of the optical conductivity of $\text{La}_{1.775}\text{Sr}_{0.225}\text{NiO}_4$ in the phonon spectral range.

The charge-stripe order is characterized (approximately [10,25]) by the wave vector $\mathbf{Q}_c = (\epsilon, \epsilon, 1)$ with $\epsilon = 0.275$, which has rotational symmetry $\mathbf{mm}2$ with the second order axis along the x' -direction. The phonon states of the average structure at \mathbf{Q}_c are distributed among the IREPs of the $\mathbf{mm}2$ wave vector group in the following manner: $7\Sigma_1(x') + 3\Sigma_2 + 5\Sigma_3(y') + 6\Sigma_4(z)$. All of these states must be Raman-active, and Σ_1 , Σ_3 , and

Σ_4 states are IR-active. The Σ_1 and Σ_3 modes must appear in $x'x'$ and $x'y'$ RLS spectra, respectively, if charge ordering creates lattice distortions belonging to the Σ_1 IREP. Intensities of these new lines depend strongly on the type and symmetry of the modes, and on the nature of the electron-phonon coupling. Stripe order perturbations of the dynamical phonon matrix must also lead to a lowering of the rotational symmetry of the phonon states at $\mathbf{Q} = 0$ from the D_{4h} group to the C_{2v} group, and to a splitting of the two-fold degenerate E -states.

To identify the new peaks induced by stripe order, we make use of the phonon-dispersion curves determined in the neutron-scattering study of La_2NiO_4 by Pintschovius *et al.* [20]. The $Q = 0$ optically-active modes are expected to shift by only small amounts due to doping, although some hardening is expected on cooling to low temperatures, as the neutron study was performed at room temperature. Ideally, we would like to compare with the dispersion curves along $\mathbf{Q} = (\xi, \xi, 1)$; however, since measurements have not been made along that direction, we will compare with $(\xi, \xi, 0)$, and rely on the fact that dispersion along [001] is generally much smaller than in-plane dispersion [20].

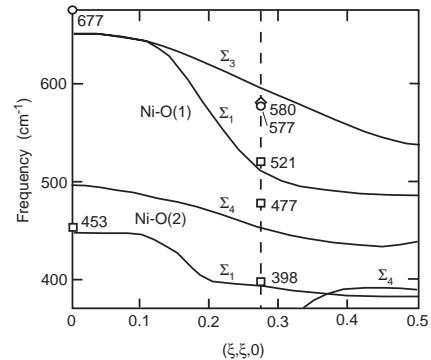


FIG. 4. Comparison of major RLS and IR features in $\text{La}_{1.775}\text{Sr}_{0.225}\text{NiO}_4$ at 5–10 K with the phonon dispersions for bond-stretching modes measured for La_2NiO_4 at room temperature [20]. Squares: Raman $x'x'$; diamonds: Raman $x'y'$; circles: IR. Dashed line indicates charge-order wave vector, \mathbf{Q}'_c .

In Fig. 4, we show the highest-energy phonon branches along $(\xi, \xi, 0)$ from Ref. [20]. The two upper branches involve Ni-O(1) (in-plane) bond-stretching motions, while the lower two derive from Ni-O(2) (c -axis) bond-stretching. The dashed line indicates the in-plane charge-ordering wave vector $\mathbf{Q}'_c = (\epsilon, \epsilon, 0)$. In the following, we will associate the new features in the RLS and IR spectra induced by charge order with \mathbf{Q}'_c .

Starting with the Raman $x'x'$ spectra (Fig. 2), we observe that, at 150 K and below, several peaks appear in the vicinity of the native Ni-O(2) bond-stretching mode, which occurs at 447 cm^{-1} for $x = 0$. A somewhat similar set of split peaks was observed for $x = \frac{1}{3}$ in the charge-ordered phase [18,19]. For $x = 0.225$, significant peaks

appear at 398, 453, 477, and 521 cm^{-1} . We attribute the 453 cm^{-1} feature to the $Q = 0$ mode, and the 398 cm^{-1} peak to the \mathbf{Q}'_c mode, on the Σ_1 branch involving the already-noted Ni-O(2) motion. The 477 cm^{-1} peak appears to be close to the Σ_4 branch, which would require electron-phonon coupling to make it Raman active. In contrast, the 521 cm^{-1} peak is too high in energy to involve Ni-O(2) motion (contrary to the speculation in Ref. [18]). It must correspond to the \mathbf{Q}'_c mode of the highest Σ_1 branch, which involves Ni-O(1) bond-stretching motion.

For the Raman $x'y'$ spectra, there is a temperature-dependent peak at 580 cm^{-1} . Symmetry arguments, together with the frequency, indicate that this is the \mathbf{Q}'_c mode of the highest Σ_3 branch, which also involves Ni-O(1) bond-stretching motion.

Finally, we arrive at the optical conductivity (Fig. 3). The peak at 356 cm^{-1} corresponds to the native E_u mode involving Ni-O(1)-Ni bond-bending motion. It was observed to split into at least 3 peaks in the charge-ordered phase of $x = \frac{1}{3}$ [2]. The total splitting is comparable to the width of our peaks. Model calculations that we have performed using a modified rigid-ion model indicate that the splitting and shifts of these peaks should be sensitive to the way in which the stripes are positioned with respect to the lattice. The lack of a clear splitting in the present case may indicate the absence of a unique positioning of the stripes, which would be consistent with the incommensurate wave vector and the finite correlation length for stripe order. Our calculations suggest that the peak at 677 cm^{-1} (corresponding to the 654 cm^{-1} peak at $x = 0$) should also be sensitive to stripe pinning, but, again, no clear splitting is observed.

The most unusual feature in Fig. 3 is the strong dip at 577 cm^{-1} . Because of the unusual nature of this apparent Fano antiresonance, the measurement of the reflectivity in this frequency range was repeated several times with different detectors and scanning rates in order to verify that it is not an artifact. The occurrence of a dip instead of a peak clearly indicates interference of a phonon mode with underlying electronic conductivity. The energy of this feature uniquely associates it with Ni-O(1) stretching motion.

Model calculations for stripes in a NiO_2 plane using the inhomogeneous Hartree-Fock plus random-phase-approximation approach by Yi *et al.* [26] have demonstrated how the modulation of electronic hybridization by Ni-O(1) bond-stretching modes results in extra phonon branches and strong new IR modes. Our antiresonance mode is undoubtedly of this type. The model calculations were done for stripes with a hole density of one per Ni site, resulting in a large charge excitation gap [26]. In contrast, for our $x = 0.225$ sample the hole density per Ni site along a stripe is $x/\epsilon = 0.225/0.275 = 0.82$, which is consistent with a quasi-metallic character. The antiresonant behavior demonstrates the existence of a finite con-

ductivity within the charge stripes at energies well below the pseudogap (0.105 eV), which is presumably associated with charge motion transverse to the stripes. The continued existence of the antiresonance at room temperature, well above T_c , suggests that stripe correlations do not disappear at T_c . Such a result should not be too surprising given that the low-frequency conductivity remains small well above T_c , indicating the continuing importance of strong correlations. The occurrence of stripe correlations without static order has significant implications for understanding the cuprates.

This work was supported in part by INTAS grant No. 96-0410 and DFG/SFB 341 and SFFR research grant No. 2.4/247 of Ukraine. JMT is supported by U.S. DOE Contract No. DE-AC02-98CH10886.

-
- [1] T. Ido, K. Magoshi, H. Eisaki, and S. Uchida, Phys. Rev. B **44**, 12094 (1991).
 - [2] T. Katsufuji *et al.*, Phys. Rev. B **54**, R14230 (1996).
 - [3] C. H. Chen, S.-W. Cheong, and A. S. Cooper, Phys. Rev. Lett. **71**, 2461 (1993).
 - [4] J. M. Tranquada, D. J. Buttrey, V. Sachan, and J. E. Lorenzo, Phys. Rev. Lett. **73**, 1003 (1994).
 - [5] S.-H. Lee and S.-W. Cheong, Phys. Rev. Lett. **79**, 2514 (1997).
 - [6] S. Tajima *et al.*, J. Phys. Chem. Solids **59**, 2015 (1998).
 - [7] J. M. Tranquada *et al.*, Nature **375**, 561 (1995).
 - [8] M. v. Zimmermann *et al.*, Europhys. Lett. **41**, 629 (1998).
 - [9] J. M. Tranquada *et al.*, Phys. Rev. B **54**, 7489 (1996).
 - [10] J. M. Tranquada, D. J. Buttrey, and V. Sachan, Phys. Rev. B **54**, 12318 (1996).
 - [11] A. Vighiante *et al.*, Phys. Rev. B **56**, 8248 (1997).
 - [12] J. M. Tranquada *et al.*, Phys. Rev. Lett. **78**, 338 (1997).
 - [13] J. E. Ostenson *et al.*, Phys. Rev. B **56**, 2820 (1997).
 - [14] H. Eskes *et al.*, Phys. Rev. B **58**, 6963 (1998).
 - [15] S. A. Kivelson, E. Fradkin, and V. J. Emery, Nature **393**, 550 (1998).
 - [16] A. P. Ramirez *et al.*, Phys. Rev. Lett. **76**, 447 (1996).
 - [17] R. J. McQueeney, J. L. Sarrao, and R. Osborn, Phys. Rev. B **60**, 80 (1999).
 - [18] G. Blumberg, M. V. Klein, and S. W. Cheong, Phys. Rev. Lett. **80**, 564, (1998).
 - [19] K. Yamamoto, T. Katsufuji, T. Tanabe, and Y. Tokura, Phys. Rev. Lett. **80**, 1493 (1998).
 - [20] L. Pintschovius *et al.*, Phys. Rev. B **40**, 2229 (1989).
 - [21] G. Burns *et al.*, Phys. Rev. B **42**, 19777 (1990).
 - [22] S. Sugai *et al.*, Physica C **185-189**, 895 (1991).
 - [23] D. E. Rice, M. K. Crawford, D. J. Buttrey, and W. E. Farneth, Phys. Rev. B **42**, 8787 (1990).
 - [24] S. Tajima *et al.*, Phys. Rev. B **43**, 10496 (1991).
 - [25] P. Wochner, J. M. Tranquada, D. J. Buttrey, and V. Sachan, Phys. Rev. B **57**, 1066 (1998).
 - [26] Y.-S. Yi, Z.-G. Yu, A. R. Bishop, and J. T. Gammel, Phys. Rev. B **58**, 503 (1998).